CT-based radiomics signature of visceral adipose tissue for prediction of disease progression in patients with Crohn's disease: A multicentre cohort study

Xuehua Li,[a,k] Naiwen Zhang,[b,k] Cicong Hu,[a,k] Yuqin Lin,[c,k] Jiaqiang Li,[d] Zhoulei Li,[a] Enming Cui,[e] Li Shi,[f] Xiaozhao Zhuang,[g] Jianpeng Li,[h] Jiahang Lu,[i] Yangdi Wang,[a] Renyi Liu,[a] Chenglang Yuan,[b] Haiwei Lin,[b] Jinshen He,[j] Dongping Ke,[c] Shanshan Tang,[d] Yujian Zou,[h] Bo He,[i] Canhui Sun,[a] Minhu Chen,[j] Bingsheng Huang,[b,***] Ren Mao,[j,**] and Shi-Ting Feng[a,*]

[a]Department of Radiology, The First Affiliated Hospital, Sun Yat-Sen University, 58 Zhongshan II Road, Guangzhou 510080, People's Republic of China
[b]Medical AI Lab, School of Biomedical Engineering, Medical School, Shenzhen University, Shenzhen 518000, People's Republic of China
[c]Department of Radiology, The First Affiliated Hospital of Shantou University Medical College, 57 Changping Road, Shantou, Guangdong 515000, People's Republic of China
[d]Department of Radiology, The First People's Hospital of Foshan City, No.81, Lingnan Dadao North, Foshan City, Guangdong Province 528000, People's Republic of China
[e]Department of Radiology, Jiangmen Central Hospital, Guangdong Medical University, 23 Beijie Haibang Street, Jiangmen 529030, People's Republic of China
[f]Department of Radiology, The Third Affiliated Hospital of Guangzhou Medical University, 63 Duobao Road, Guangzhou 510150, People's Republic of China
[g]Department of Radiology, Hainan General Hospital (Hainan Affiliated Hospital of Hainan Medical University), No.19 Xiuhua Road, Xiuying District, Haikou, Hainan 570311, People's Republic of China
[h]Department of Radiology, Affiliated Dongguan People's Hospital, Southern Medical University, No. 78 Wandao Road, Gongguan 523000, People's Republic of China
[i]Medical Imaging Department, The First Affiliated Hospital, Kunming Medical University, Xi Chang Road 295th, Kunming 650000, People's Republic of China
[j]Department of Gastroenterology, The First Affiliated Hospital, Sun Yat-Sen University, 58 Zhongshan II Road, Guangzhou 510080, People's Republic of China

eClinicalMedicine 2023;56: 101805
Published Online xxx https://doi.org/10.1016/j.eclinm.2022.101805

Summary

Background **Visceral adipose tissue (VAT) is involved in the pathogenesis of Crohn's disease (CD). However, data describing its effects on CD progression remain scarce. We developed and validated a VAT-radiomics model (RM) using computed tomography (CT) images to predict disease progression in patients with CD and compared it with a subcutaneous adipose tissue (SAT)-RM.**

Methods **This retrospective study included 256 patients with CD (training, n = 156; test, n = 100) who underwent baseline CT examinations from June 19, 2015 to June 14, 2020 at three tertiary referral centres (The First Affiliated Hospital of Sun Yat-Sen University, The First Affiliated Hospital of Shantou University Medical College, and The First People's Hospital of Foshan City) in China. Disease progression referred to the development of penetrating or stricturing diseases or the requirement for CD-related surgeries during follow-up. A total of 1130 radiomics features were extracted from VAT on CT in the training cohort, and a machine-learning–based VAT-RM was developed to predict disease progression using selected reproducible features and validated in an external test cohort. Using the same modeling methodology, a SAT-RM was developed and compared with the VAT-RM.**

Abbreviations: AUC, Area under the ROC curve; BMI, Body mass index; CD, Crohn's disease; CI, Confidence interval; CRP, C-reactive protein; CT, Computed tomography; DCA, Decision curve analysis; ICC, Intraclass correlation coefficients; LASSO, Least absolute shrinkage and selection operator; LOOCV, Leave-one-out cross-validation; MRI, Magnetic resonance imaging; RM, Radiomics model; ROC, Receiver operating characteristic; SAT, Subcutaneous adipose tissue; SVM, Support vector machine; VAT, Visceral adipose tissue; VOI, Volume of interest

*Corresponding author. Department of Radiology, The First Affiliated Hospital, Sun Yat-Sen University, 58 Zhongshan Road 2nd, Guangzhou 510080, People's Republic of China.
**Corresponding author. Department of Gastroenterology, The First Affiliated Hospital, Sun Yat-Sen University, 58 Zhongshan Road 2nd, Guangzhou 510080, People's Republic of China.
***Corresponding author. Medical AI Lab, School of Biomedical Engineering, Medical School, Shenzhen University. Block A2, Xili Campus of Shenzhen University, 1066 Xueyuan Avenue, Shenzhen 518000, People's Republic of China.
E-mail addresses: fengsht@mail.sysu.edu.cn (S.-T. Feng), maor5@mail.sysu.edu.cn (R. Mao), huangb@szu.edu.cn (B. Huang).
[k]These four authors contributed equally to this work.

Findings The VAT-RM exhibited satisfactory performance for predicting disease progression in total test cohort (the area under the ROC curve [AUC] = 0.850, 95% confidence Interval [CI] 0.764–0.913, $P < 0.001$) and in test cohorts 1 (AUC = 0.820, 95% CI 0.687–0.914, $P < 0.001$) and 2 (AUC = 0.871, 95% CI 0.744–0.949, $P < 0.001$). No significant differences in AUC were observed between test cohorts 1 and 2 ($P = 0.673$), suggesting considerable efficacy and robustness of the VAT-RM. In the total test cohort, the AUC of the VAT-RM for predicting disease progression was higher than that of SAT-RM (AUC = 0.786, 95% CI 0.692–0.861, $P < 0.001$). On multivariate Cox regression analysis, the VAT-RM (hazard ratio [HR] = 9.285, $P = 0.005$) was the most important independent predictor, followed by the SAT-RM (HR = 3.280, $P = 0.060$). Decision curve analysis further confirmed the better net benefit of the VAT-RM than the SAT-RM. Moreover, the SAT-RM failed to significantly improve predictive efficacy after it was added to the VAT-RM (integrated discrimination improvement = 0.031, $P = 0.102$).

Interpretation Our results suggest that VAT is an important determinant of disease progression in patients with CD. Our VAT-RM allows the accurate identification of high-risk patients prone to disease progression and offers notable advantages over SAT-RM.

Funding This study was supported by the National Natural Science Foundation of China, Guangdong Basic and Applied Basic Research Foundation, Shenzhen-Hong Kong Institute of Brain Science-Shenzhen Fundamental Research Institutions, Nature Science Foundation of Shenzhen, and Young S&T Talent Training Program of Guangdong Provincial Association for S&T.

Translation For the Chinese translation of the abstract see Supplementary Materials section.

Keywords: Crohn's disease; Visceral adipose tissue; Radiomics; Computed tomography enterography

Research in context

Evidence before this study

Visceral adipose tissue (VAT) is involved in the pathogenesis of Crohn's disease (CD). However, tools uncovering the pathophysiological changes within VAT are limited and data describing its effects on disease progression in CD remain scarce. Radiomics, a powerful tool for quantitative analysis of medical images, can describe visually unrecognizable tissue heterogeneity as well as substantial differences between pathological and normal VAT. We searched PubMed and Web of Science for the terms ("Crohn's disease", "Inflammatory bowel disease", "Visceral adipose tissue", "Creeping fat", "Disease progression", "Radiomics", "Texture analysis", "Machine learning", "Computed tomography", or "Cross-sectional imaging") up to September 1, 2022, with no language restrictions. No study has investigated the efficacy of computed tomography images based radiomics analysis for predicting disease progression in patients with CD.

Added value of this study

To our best knowledge, this is the first multicenter radiomics study to evaluate the effect of the whole VAT on CD progression. VAT is recognized as an important determinant of disease progression in CD according to our radiomics results. Our VAT-based radiomics model allows accurate identification of patients with CD who were prone to show disease progression. Importantly, the model is robust across different treatment centers.

Implications of all the available evidence

Our radiomics results reinforce the knowledge of the potential mechanisms underlying the effects of VAT on adverse intestinal outcomes in CD, this approach can serve as a supplement to current risk stratification strategies at no extra expense since computed tomography examination is routinely performed in clinical practice.

Introduction

Early stratification of patients with Crohn's disease (CD) according to the risk of strictures, penetrating diseases, or surgery is the most optimal and cost-effective approach to tailor therapy for this disease.[1] Increasing data have shown that visceral adipose tissue (VAT) is involved in the pathogenesis of CD and increases the risk of development.[2] Mesenteric VAT and intestines have recently been considered to affect each other when disease occurs.[3] In CD, hypertrophied mesenteric VAT (so-called 'creeping fat') can be present as early as the onset of intestinal inflammation,[4] so it is a sensitive sign

of complications.[5] In contrast, limited data showed an obscure role of subcutaneous adipose tissue (SAT) in CD.[6] Thus, VAT may be a more powerful predictor of CD progression.

Although the adverse effects of VAT on CD outcomes have been studied extensively, data on the usage of VAT to identify high-risk patients are scarce. Computed tomography (CT) enables the exact differentiation of VAT and SAT by measuring adipose tissue based on the fat attenuation and then establishing various fat metrics (e.g., VAT/SAT area ratio).[5] Nevertheless, studies using these fat metrics to describe the relationship between VAT and disease progression are limited, and have yielded conflicting results.[7] In comparison with indices that only reflect adipose tissue size, the dramatic disorganised microstructure and dysfunction in VAT may play a superior role in studying the pathogenesis and therapeutic response of CD.[8]

CT imaging can clearly capture these pathophysiological changes within VAT.[9] Radiomics, a novel tool for high-throughput extraction of quantitative features from medical images, can describe visually unrecognizable tissue heterogeneity as well as substantial differences between pathological and normal VAT. Recently, we have successfully characterised bowel fibrosis in CD using a CT-based radiomics approach.[10] Moreover, CT radiomics signatures of epicardial or peri-coronary adipose tissue show the feasibility of using radiomics analysis for providing clinical-decision support.[11,12]

To our best knowledge, few studies have reported whether the radiomics signature of VAT enables superior prediction of CD progression. Herein, we used CT data collected from three centres to develop and validate a VAT-based radiomics model (RM) for predicting disease progression in patients with CD and compared its capability with SAT-based RM and six conventional fat metrics (VAT/SAT area ratio, etc.).

Methods

Patients and study design

In this retrospective multicentre study, 382 patients with CD who underwent baseline CT enterography were consecutively recruited from three tertiary referral centres in China from June 19, 2015 to June 14, 2020. This study was approved by the institutional ethics review boards of all participating hospitals, which waived the requirement for obtaining informed consent. Patients with CD from The First Affiliated Hospital of Sun Yat-Sen University comprised the training cohort for developing the RMs. To test the predictive performance of the RMs, we further enrolled patients with CD from The First Affiliated Hospital of Shantou University Medical College and The First People's Hospital of Foshan City to constitute test cohorts 1 and 2, respectively (Fig. 1). The training cohort included 156 patients, and the total test cohort enrolled 100 patients (test cohort 1, n = 51; test cohort 2, n = 49). The baseline demographic and clinical characteristics of the patients in the training and total test cohorts are shown in Table 1.

The inclusion criteria were as follows: *(a)* patients with CD with Montreal B1 at baseline; *(b)* available complete clinical data within one week of CT enterography at baseline; and *(c)* a follow-up of at least 6 months for patients without disease progression. The exclusion criteria were as follows: *(a)* penetrating diseases, stricturing diseases, prior bowel resection history, or consideration of CD-related surgery on initial admission; *(b)* VAT/SAT not readily identifiable on CT due to severe abdominal/pelvic effusion or subcutaneous oedema; *(c)* concomitant malignant tumours or metabolic diseases (e.g., hyperthyroidism or diabetes) that could affect the distribution or function of adipose tissue; and *(d)* use of corticosteroids and biologics within three months prior to enrolment.[13]

Collection of clinical and laboratory data

Baseline and follow-up data of patients, such as C-reactive protein (CRP) and albumin levels, were collected from the electronic medical records; the details are shown in Table 1. Among them, the use of biologics at baseline and during follow-up was defined as the use of dosing for induction or maintenance[14]; the use of corticosteroids was defined as the use of a systemic corticosteroid, either orally or intravenously administered[15]; and the use of an immunomodulator was defined if its use was documented for more than 3 months.[16]

Follow-up and disease progression definition

During follow-up, disease progression was defined as the development of penetrating or stricturing diseases, or the need for CD-related surgery; other cases were categorised as showing non-disease progression. Penetrating diseases included intestinal fistulae, inflammatory masses or abscesses[17] that were detected on CT, magnetic resonance imaging (MRI), or ultrasonography (Supplementary Table S1). Stricturing disease was defined as intestinal strictures with upstream dilatation detected on cross-sectional imaging,[18] with or without clinical obstruction symptoms. CD-related surgery included bowel resection and strictureplasty but not appendectomy or anal fistula surgery. The indications for surgery included intestinal penetrating diseases, stricturing diseases, and medically refractory diseases. If surgery was performed due to the occurrence of penetrating or stricturing diseases in the same period, the adverse outcome was only recorded as surgery.

The assessment of disease progression in each centre was performed using outpatient/inpatient data by

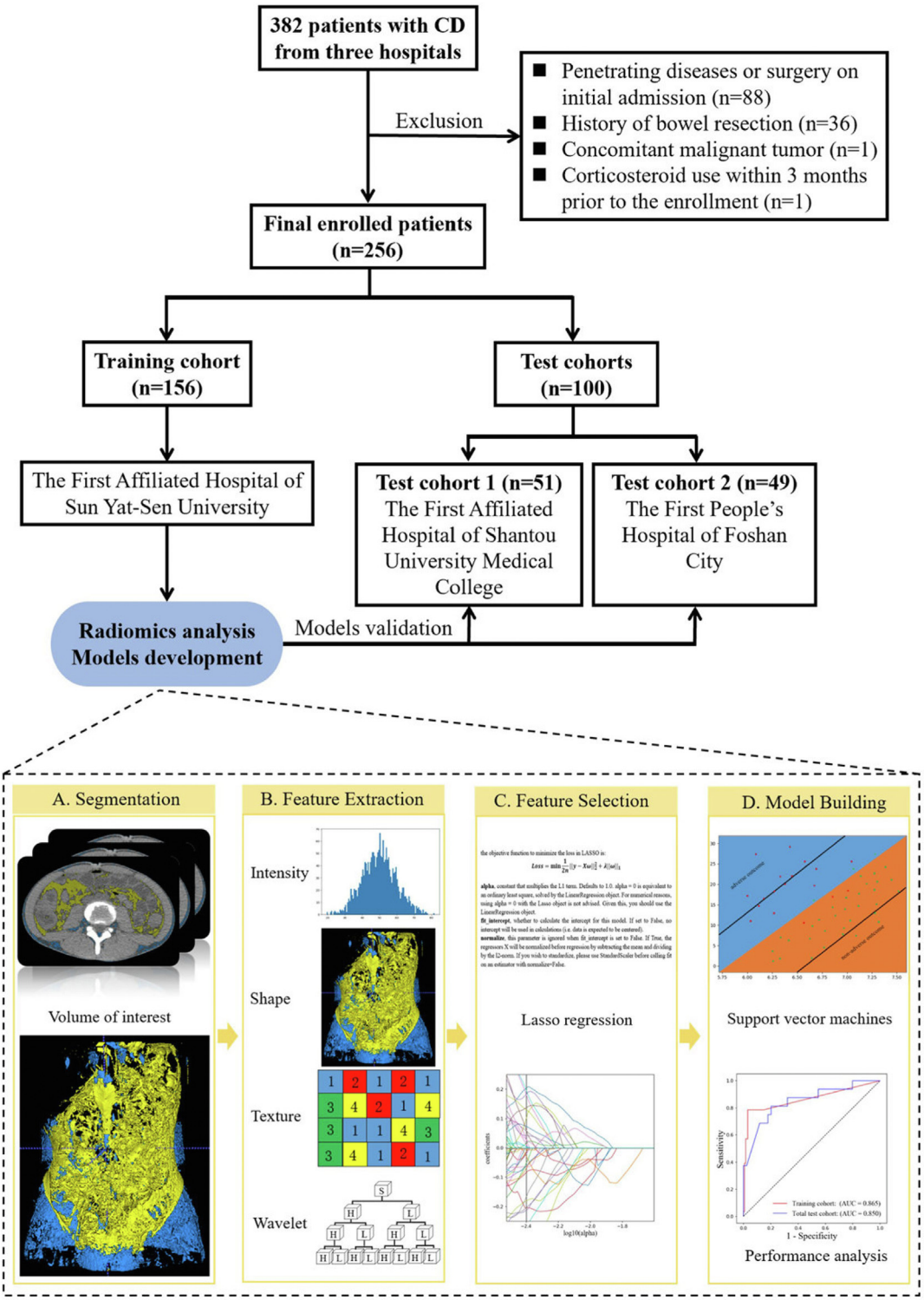

Fig. 1: Flow diagram of the study population and the radiomics workflow. (CD, Crohn's disease).

Characteristics	Training cohort (n = 156)			Total test cohort (n = 100)		
	Disease progression (n = 28)	Non-disease progression (n = 128)	*P* value	Disease progression (n = 16)	Non-disease progression (n = 84)	*P* value
Disease progression, n (%)[a]						
Penetrating diseases	10 (35.71%)			5 (31.25%)		
Bowel obstruction	14 (50.00%)			5 (31.25%)		
Surgery	4 (14.29%)			6 (37.50%)		
Follow-up time (months)[d]	21.68 (14.72, 28.64)	25.88 (23.85, 27.90)	0.134	18.81 (9.58, 28.05)	28.52 (25.51, 31.53)	0.009
Clinical factors at baseline						
Sex, n (%)[a]			0.365			0.242
Male	17 (60.71%)	89 (69.53%)		12 (75.00%)	50 (59.52%)	
Female	11 (39.29%)	39 (30.47%)		4 (25.00%)	34 (40.48%)	
Age[c]	25.50 (20.50, 40.00)	28.00 (20.00, 34.00)	0.757	34.00 (23.50, 47.25)	26.00 (22.00, 34.00)	0.141
Disease location[a]			0.718			0.243
L1 [ileal]	7 (25.00%)	32 (25.00%)		2 (12.50%)	29 (34.52%)	
L2 [colonic]	1 (3.57%)	5 (3.91%)		0 (0.00%)	5 (5.95%)	
L3 [ileocolonic]	18 (64.29%)	69 (53.91%)		11 (68.75%)	38 (45.24%)	
L4 [upper]	0 (0.00%)	1 (0.78%)		0 (0.00%)	0 (0.00%)	
L1+L4	1 (3.57%)	3 (2.34%)		1 (6.25%)	7 (8.33%)	
L2+L4	0 (0.00%)	0 (0.00%)		0 (0.00%)	0 (0.00%)	
L3+L4	1 (3.57%)	18 (14.06%)		2 (12.50%)	5 (5.95%)	
Smoking, n (%)[a,e]	2 (7.14%)	14 (10.94%)	0.568	2 (12.50%)	6 (7.14%)	0.861
Disease duration (months)[c]	24.00 (10.50, 48.00)	12.00 (5.00, 48.00)	0.148	12.50 (9.75, 48.00)	12.00 (2.00, 36.00)	0.259
BMI (kg/m^2)[c]	17.70 (16.44, 20.20)	18.92 (17.11, 20.93)	0.089	18.69 (15.07, 21.68)	17.95 (15.61, 19.30)	0.304
Perianal fistula/abscess[a]	14 (50.00%)	59 (46.09%)	0.707	0 (0.00%)	13 (15.48%)	0.092
Medicine use at baseline, n (%)[a]						
Biologics use 3 months ago	1 (3.57%)	2 (1.56%)	0.483	3 (18.75%)	6 (7.14%)	0.137
Corticosteroids use 3 months ago	3 (10.71%)	10 (7.81%)	0.615	1 (6.25%)	7 (8.33%)	0.778
Immunomodulator	4 (14.29%)	15 (11.72%)	0.707	3 (18.75%)	6 (7.14%)	0.137
Medicine use during follow-up, n (%)[a]						
Biologics	14 (50.00%)	77 (60.16%)	0.323	9 (56.25%)	50 (59.52%)	0.807
Corticosteroids	12 (42.86%)	31 (24.22%)	0.046	7 (43.75%)	26 (30.95%)	0.318
Immunomodulator	17 (60.71%)	68 (53.12%)	0.465	9 (56.25%)	44 (42.38%)	0.776
Laboratory factors at baseline						
CRP (mg/L)[c]	20.00 (8.74, 43.85)	14.10 (3.92, 28.80)	0.076	14.59 (7.92, 55.78)	17.10 (5.25, 46.75)	0.560
ESR (mm/h)[c]	40.00 (20.25, 58.75)	32.00 (13.00, 61.00)	0.672	27.00 (18.75, 53.25)	28.00 (14.00, 48.00)	0.603
Albumin (g/L)	34.96 ± 5.41[b]	35.91 ± 5.66[b]	0.429	33.05 (24.75, 37.10)[c]	35.52 (31.03, 40.78)[c]	0.075
Hemoglobin (g/L)[b]	109.61 ± 22.64	116.49 ± 23.67	0.164	110.01 ± 28.36	112.30 ± 23.22	0.348
Platelet (×10^9/L)[c]	336.00 (278.00, 415.25)	340.00 (261.00, 427.00)	0.873	294.50 (244.75, 464.75)	347.50 (255.50, 419.00)	0.873
Endoscopic ulcer at baseline, n (%)[a]			0.922			0.120
None	3 (10.71%)	16 (12.50%)		4 (25.00%)	7 (8.33%)	
Superficial ulcer	13 (46.43%)	62 (48.44%)		4 (25.00%)	34 (40.48%)	
Deep ulcer	12 (42.86%)	50 (39.06%)		8 (50.00%)	43 (51.19%)	

P < 0.050 was considered statistical significance. BMI, body mass index; CRP, C-reactive protein; ESR, erythrocyte sedimentation rate. [a]Categorical variables, expressed as frequencies (proportions), line χ^2 test. [b]Normally distributed variables, expressed as mean ± standard deviation, line independent T-test. [c]Non-normally distributed variables, expressed as median (interquartile range), line Mann–Whitney U test. [d]Numbers in parentheses are the 95% confidence interval. [e]Smoker, defined as a minimum of five cigarettes per week for at least one year in the past or at present.

Table 1: **The demographic and clinical characteristics of patients with Crohn's disease in the training and total test cohorts.**

one gastroenterologist and one radiologist (who were unaware of any information other than their allocated data) together from their own hospital. If more than one examination was performed during the follow-up, the earliest date reporting disease progression was recorded.

The follow-up endpoint was defined as the time of disease progression or March 2021 for patients without disease progression. The time from baseline to the follow-up endpoint was defined as the disease progression-free survival.

Development and validation of VAT and SAT RMs

All patients underwent baseline CT examinations using one of the five CT scanners at the three centres (Supplementary Material 1). For noninvasive assessment, plain CT images were selected for radiomics analysis. To better investigate the role of VAT, SAT was also analysed. Fig. 1 shows the workflow of the radiomics procedure.

Volume of interest segmentation and radiomics features extraction and selection

The VAT and SAT were automatically segmented on CT images (Supplementary Material 2). Subsequently, the boundaries of automatically segmented volumes of interests (VOIs) were manually reviewed and corrected for any errors by a radiologist using open-source medical imaging software (ITK-SNAP, version 3.8.0; www.itksnap.org). Radiomics features were extracted from the corrected VOIs that encompassed the VAT or SAT by using an open-source pyradiomics toolkit (https://pyradiomics.readthedocs.io/en/v1.0/installation.html). A total of 1130 radiomics features were extracted, including shape features, first-order features, texture features, and wavelet features. Unsupervised clustering and radiomics heatmaps were used to reveal clusters of similar radiomics expression patterns and their associations with adverse outcomes. More details on radiomics feature extraction are provided in Supplementary Material 3.

To evaluate the inter-/intra-observer reproducibility of the extracted features, 30 patients randomly selected from the training cohort were verified twice over a 3-month interval by another radiologist with the same tool and environment settings. Intraclass correlation coefficients (ICCs) were calculated using a two-way random effects model to determine inter-/intra-observer reliabilities.

To avoid overfitting and enhance model robustness, a two-step procedure for feature selection was performed. First, we selected features with ICCs $\geq$0.8, which were considered robust. Then, we used the least absolute shrinkage and selection operator (LASSO) of the logistic regression algorithm to determine the best subset of radiomics features. To investigate the discrepancy in adipose tissue radiomics features between adverse and non-adverse outcomes, feature maps of selected features were generated using voxel-based radiomics analysis.

Radiomics models development and validation

For the VAT-RM, a support vector machine (SVM) classifier was used to distinguish the outcome for each patient. To select the best parameters for the predictive model, the leave-one-out cross-validation (LOOCV) strategy was used in the training cohort. In the training procedure of LOOCV, a grid search method was used to determine the optimal parameters, which consisted of C (regularisation parameter), max_iter (hard limit on iterations within solver), and gamma (kernel coefficient) in the SVM model. All probabilities of testing samples in each fold during cross-validation were used to assess the prediction performance in the training cohort. In the testing procedure, all SVM models built on the training cohort were integrated with the same weight to predict the individual predictive probability for the test cohort, which was defined as the radiomic signature score. We also performed stratification analysis on the subgroups of different test cohorts and different CT scanners to assess the stability of VAT-RM. The procedure for SAT-RM development and validation was the same as that for VAT-RM.

Measurement of other imaging metrics of adipose tissue

Since VAT volume, SAT volume, VAT/SAT volume ratio, and VAT/SAT area ratio have been reported to play important roles in previous studies of adipose tissue in CD,[5,6,19,20] we included them for comparison with the RMs.

VAT volume, SAT volume, and VAT/SAT volume ratio

VAT volume (mm^3) on CT was calculated using the VOIs of VAT with the open-source pyradiomics toolkit mentioned above. SAT volume was calculated using the same approach as that used for VAT volume. VAT/SAT volume ratio was equal to VAT volume divided by SAT volume (Supplementary Fig. S1).

VAT/SAT area ratio at L3 and L4 vertebral levels

VAT and SAT areas (mm^2) at the L3 and L4 vertebral levels were automatically measured on CT using the open-source opencv-python toolkit (https://pypi.org/project/opencv-python/). VAT/SAT area ratio was equal to VAT area divided by SAT area (Supplementary Fig. S1).

Statistical analysis

Sample size evaluation

A sample size of at least 26 cases (13 disease progression and 13 non-disease progression) was required in the training and test cohorts based on the following inputs and assumptions: power, 80%; two-sided significance level, 0.05; alternative hypothesis of the area under the receiver operating characteristic (ROC) curve (AUC), 0.800, compared with the null hypothesis of the AUC, 0.500; and an allocation ratio of sample sizes in the negative and positive groups of 1. Thus, sample sizes of 156 (28 disease progression and 128 non-disease progression) in the training cohort and 100 (16 disease progression and 84 non-disease progression) in the test cohort were sufficient to detect an AUC difference of 0.500 with 80% power if the true AUC was

above 0.800. Statistical analyses were performed using MedCalc (version 20.009; https://www.medcalc.org).

Diagnostic performance

Univariate analysis for clinical factors was performed using Student's t-test, the Mann–Whitney U test, or the Chi-square test according to the data distribution. The prediction efficacies of the RMs were evaluated using the AUC, reported by calibration using the Hosmer–Lemeshow goodness-of-fit test. ROC curves between different models were compared using the DeLong test. Additionally, integrated discrimination improvement (IDI) was calculated to test the incremental predictive value of the SAT-RM after adding it to the VAT-RM. Decision curve analysis (DCA) was conducted to evaluate the clinical usefulness of the RMs by quantifying the net benefit at different threshold probabilities.

Survival analysis

The training and test cohorts were stratified into low- and high-risk subgroups according to the Youden index by the RMs. Disease-progression-free survival was assessed using the Kaplan–Meier method, and differences in survival distributions between the stratified subgroups were compared using log-rank tests. Time-dependent ROC curve and corresponding AUC were employed to investigate the performance at different time points. Clinical characteristics, two RMs, and other fat metrics were applied as candidate predictive factors and tested using univariate Cox regression analysis. To identify which factors were the independent predictors for disease-progression-free survival, multivariate Cox regression analysis was performed using factors with a *P*-value <0.100 on the univariate Cox regression analysis. The C-index between the predicted probability and actual outcome was calculated to evaluate the predictive ability of the RMs.

Statistical analyses were performed using R statistical software (version 4.1.2; https://www.r-project.org/; Supplementary Table S2) or SPSS (version 20; https://www.ibm.com/cn-zh/analytics/spss-statistics-software). A two-sided *P*-value of <0.050 was used to indicate statistical significance, except on the univariate Cox regression analysis ($P < 0.100$).

Role of the funding source

The funders of the study had no role in study design, data collection, data analysis, data interpretation, or writing of the report. All authors read, discussed, and approved the final version of the manuscript. All authors had full access to the data in the study and takes responsibility for the integrity of the data and the accuracy of the data analysis as well as the decision to submit for publication.

Results

Patient characteristics

During the follow-up period, 28 (17.9%) patients from the training cohort and 16 (16.0%) patients from the total test cohort experienced disease progression (Table 1). Among them, ten patients underwent bowel resection; the causes of surgery included penetrating or stricturing diseases detected before a selective operation (n = 5) or emergency operation (n = 2) and medically refractory disease (n = 3). The 1-, 2-, 3-, and 4-year disease progression-free survival rates were 0.923 (95% CI, 0.882–0.966), 0.874 (95% CI, 0.817–0.934), 0.755 (95% CI, 0.652–0.873), and 0.602 (95% CI, 0.460–0.788), respectively, for the training cohort and 0.906 (95% CI, 0.850–0.967), 0.864 (95% CI, 0.793–0.941), 0.837 (95% CI, 0.754–0.930), and 0.682 (95% CI, 0.487–0.954), respectively, for the total test cohort.

Development and validation of the VAT-RM

Radiomics feature selection

There were 1130 radiomics features extracted from the plain CT images per patient. Among them, 1128 features with inter-/intra-observer ICCs of ≥0.8 were retained as candidates for developing the VAT-RM. Inter-/intra-observer reproducibility of the extracted radiomics features are shown in Supplementary Table S3. Finally, 36 features were selected to build the VAT-RM based on the training cohort (Supplementary Fig. S2A; Supplementary Table S4). Heatmaps of these features and unsupervised cluster partitioning are shown in Supplementary Fig. S2B and C.

Radiomics model development

The SVM model was trained to achieve the best performance based on the training cohort and then applied to the test cohort. The output of the VAT-RM was generated as a function of a nonlinear combination of the 36 selected features. This output is a value between zero and one, denoting the predicted probability of disease progression. The formula is as follows:

$$\text{Prediction probability} = \frac{1}{1+e^{F(x)}}$$

$$F(x) = -676.580 \times f(sf) - 677.515$$

where $f(x)$ is the decision_function of SVM and sf is the selected radiomics features. The best cutoff value on the VAT-RM for discriminating patients with and without disease progression was 0.315, which divided the patients into high- and low-risk subgroups.

Predictive performance validation of the RM

In the training cohort, the VAT-RM predicted disease progression with an AUC of 0.865 (95% CI,

0.801–0.914, $P < 0.001$). In the external validation, the VAT-RM still exhibited satisfactory predictive performance in the total test cohort (AUC = 0.850, 95% CI, 0.764–0.913, $P < 0.001$) and in each individual test cohort (AUC = 0.820, 95% CI, 0.687–0.914 and AUC = 0.871, 0.744–0.949, respectively, both $P < 0.001$; Table 2).

No significant differences in AUC were observed between the training and total test cohorts ($P = 0.841$; Fig. 2A) or between test cohorts 1 and 2 ($P = 0.673$; Fig. 2B), suggesting considerable efficacy and robustness of the VAT-RM. The Hosmer–Lemeshow test yielded χ^2 values of 0.088 ($P = 0.957$) and 3.590 ($P = 0.166$) in the training and total test cohorts, respectively, indicating a good VAT-RM fit (Fig. 2C). The AUC of the VAT-RM from CT scanners 1–5 ranged from 0.820 to 0.916 (Supplementary Table S5). There were no significant differences in the AUC of the VAT-TM among different CT scanners (all $P > 0.05$; Supplementary Table S6), further indicating its remarkable robustness.

Development and validation of the SAT-RM

Using the same modelling process as the VAT-RM, 1130 radiomics features were initially extracted from SAT; among them, 1118 features with inter/intra-observer ICCs of ≥0.8 were retained as candidates. Finally, 35 features were selected to develop the SAT-RM (Supplementary Table S3; Supplementary Fig. S2D–F; Supplementary Table S7). The formula is as follows:

$$\text{Prediction probability} = \frac{1}{1+e^{F(x)}}$$

$$F(x) = -2.021 \times f(sf) - 2.939$$

where $f(x)$ is the decision_function of SVM and sf is the selected radiomics features. The best cutoff value of the SAT-RM was 0.543, which divided patients into high- and low-risk subgroups.

No significant differences in the AUC of the SAT-RM for predicting disease progression were observed between the training cohort (AUC = 0.824, 95% CI, 0.755–0.880, $P < 0.001$) and the total test cohort (AUC = 0.786, 95% CI, 0.692–0.861, $P < 0.001$) ($P = 0.652$; Fig. 2D) and between test cohorts 1 (AUC = 0.741, 95% CI, 0.599–0.853, $P = 0.022$) and 2 (AUC = 0.803, 95% CI, 0.664–0.903, $P = 0.017$) ($P = 0.707$; Fig. 2E, Table 2). The Hosmer–Lemeshow test yielded χ^2 values of 4.152 ($P = 0.125$) and 0.824 ($P = 0.663$) in the training and total test cohorts, respectively, suggesting a good SAT-RM fit (Fig. 2F). There were no significant differences in the AUC of the SAT-RM among different CT scanners (all $P > 0.05$; Supplementary Tables S5 and S6).

Comparison of predictive performance between the VAT-RM and SAT-RM

The VAT-RM demonstrated superior predictive performance for disease progression compared to the SAT-RM in the training cohort (AUC = 0.865 vs. AUC = 0.824, $P = 0.532$; Fig. 2G) and in the total test cohort (AUC = 0.850 vs. AUC = 0.786, $P = 0.323$; Fig. 2H), although these differences were not significant. Moreover, time-dependent ROC analysis demonstrated the prediction performance of the two RMs at 1, 2, 3, and 4 years, revealing higher AUCs for the VAT-RM than for the SAT-RM at most of the time points in both cohorts (Supplementary Fig. S3A–D).

Since the SAT-RM showed a certain predictive efficiency, we further determined whether it provided incremental value. After adding the SAT-RM to the VAT-RM (Model 1) to construct Model 2, Model 2 failed to dramatically improve the prediction efficacy compared to Model 1 in the training cohort (IDI = 0.138, $P = 0.002$) and the total test cohort (IDI = 0.031, $P = 0.102$). Additionally, the DCA in both cohorts showed that the VAT-RM provided a better net benefit in predicting disease progression than the SAT-RM (Fig. 2I and J). Fig. 3 shows images of representative patients with or without disease progression on relevant VAT and SAT radiomics feature maps overlaid on CT images, indicating that VAT plays a more important role in the disease progression of CD than SAT.

Discriminatory performance of other metrics of adipose tissue

Between patients with and without disease progression, no significant differences were found in the six fat metrics (body mass index [BMI], VAT volume, SAT volume, VAT/SAT volume, and the VAT/SAT area ratios at the levels of L3 and L4) in the training and total test cohorts ($P = 0.089$–0.996; Supplementary Table S8).

Identification of independent predictors of disease progression

Using the VAT-RM to stratify prognostic risk, the median disease-progression-free survival of high-risk patients was significantly shorter than that of low-risk patients in the training cohort ($P < 0.001$) and total test cohort ($P < 0.001$), according to the Kaplan–Meier curves (Fig. 4A and B). Similar results were observed between high-risk and low-risk patients stratified by the SAT-RM in both cohorts (both $P < 0.001$; Fig. 4C and D).

Among all baseline and follow-up factors, VAT-RM, SAT-RM, and albumin level were identified as independent predictors by univariate Cox regression analysis with a P-value of <0.100 and were entered into the multivariate Cox regression analysis. Ultimately, VAT-RM (hazard ratio [HR] = 12.515, $P < 0.001$ in the training cohort; HR = 9.285, $P = 0.005$ in the total test

	AUC (95% CI)	Sensitivity	Specificity	Accuracy	*P* value
Training cohort					
VAT-RM	0.865 (0.801, 0.914)	0.786	0.969	0.936	<0.001
SAT-RM	0.824 (0.755, 0.880)	0.607	0.922	0.865	<0.001
Test cohort					
VAT-RM	0.850 (0.764, 0.913)	0.813	0.798	0.800	<0.001
Test cohort 1	0.820 (0.687, 0.914)	0.889	0.667	0.706	<0.001
Test cohort 2	0.871 (0.744, 0.949)	0.714	1.000	0.959	<0.001
SAT-RM	0.786 (0.692, 0.861)	0.750	0.714	0.720	<0.001
Test cohort 1	0.741 (0.599, 0.853)	0.778	0.714	0.725	0.022
Test cohort 2	0.803 (0.664, 0.903)	0.571	1.000	0.939	0.017

P value is the significance level of comparison of AUC with that of random case (AUC = 0.500). AUC, area under ROC curve; CI, confidence interval; RM, radiomic model; SAT, subcutaneous adipose tissue; VAT, visceral adipose tissue.

Table 2: **Prediction performance of VAT-RM and SAT-RM.**

cohort) was identified as the most important independent predictor of disease progression, followed by SAT-RM (HR = 2.189, $P = 0.086$ in the training cohort; HR = 3.280, $P = 0.060$ in the total test cohort) with *P*-values approaching, although not reaching, significance (Table 3). This multivariate model indicated favourable prediction of disease progression with a C-index of 0.888 and 0.863 in the training and total test cohorts, respectively.

Discussion

We used baseline CT data to develop and validate a VAT-RM for identifying patients with CD at high-risk of disease progression. Our study demonstrated that our VAT-RM can accurately predict CD progression, showing remarkable robustness in agreement among the three institutions. Although the SAT-RM demonstrated some predictive ability, its efficiency was inferior to the VAT-RM and failed to provide dramatically incremental value. Additionally, the VAT-RM significantly outperformed conventional fat metrics in predicting disease progression.

Current knowledge of the exact role of VAT in CD is still limited. Our study was designed to fill this gap, and it revealed that VAT exerted a net pathogenic effect on the intestines and thus had a close relationship with bowel disease progression. This result was supported by many studies in which creeping fat and intestinal stricturing or fistulizing complications were tightly coupled.[4,8] The secretion of pro-inflammatory mediators stimulated by gut microbiota in VAT may aggravate intestinal destruction.[21] Our VAT-RM probably captured these pathophysiological changes occurring in VAT and successfully converted them into 36 radiomics features. These radiomics features were associated with a more aggressive disease course, thus allowing the identification of high-risk patients with disease progression. Although some medications (biologics and immunomodulators) might mitigate the development of disease progression,[22] it can only be observed during a long enough follow-up period; moreover, the use of medicine was similar between the two subgroups at baseline and during follow-up in this study, further confirming the predictive role of the VAT-RM. Our radiomics results reinforced the knowledge of potential mechanisms for the effect of VAT on adverse outcomes of intestines and were essential for the selection of the most appropriate monitoring strategy for patients with CD.

To explore the effect of SAT on CD, radiomics analyses were performed. Our study showed that the SAT-RM had some predictive efficiency for disease progression. However, it was inferior to the VAT-RM and failed to provide dramatic incremental value for predicting disease progression. This result was interpretable because SAT and VAT may display distinct metabolic and immunological profiles.[2] The morphology and molecular profiles of SAT are more similar between patients with CD and healthy participants.[23]

Furthermore, a high BMI was not consistently associated with an increased prevalence of CD-related adverse outcomes[24] since the rising prevalence of obesity in patients with CD parallels the global obesity epidemic.[2] Similarly, although some studies reported that the other five fat metrics correlated with various CD complications such as penetrating diseases, strictures, or surgery,[5,6,19,25] these correlations were not found in other reports[7,26] nor in our study. This discrepancy probably reflects the shortcomings of using conventional fat metrics to predict disease progression since they only provide information about adipose tissue quantity, while its quality may play a more important role in disease diagnosis and prognosis. Similar phenomena have been described in the studies of nonalcoholic fatty liver disease and sleep apnoea, in which VAT density or metabolic activity played a more important role than adipose tissue quantity.[27,28] Before

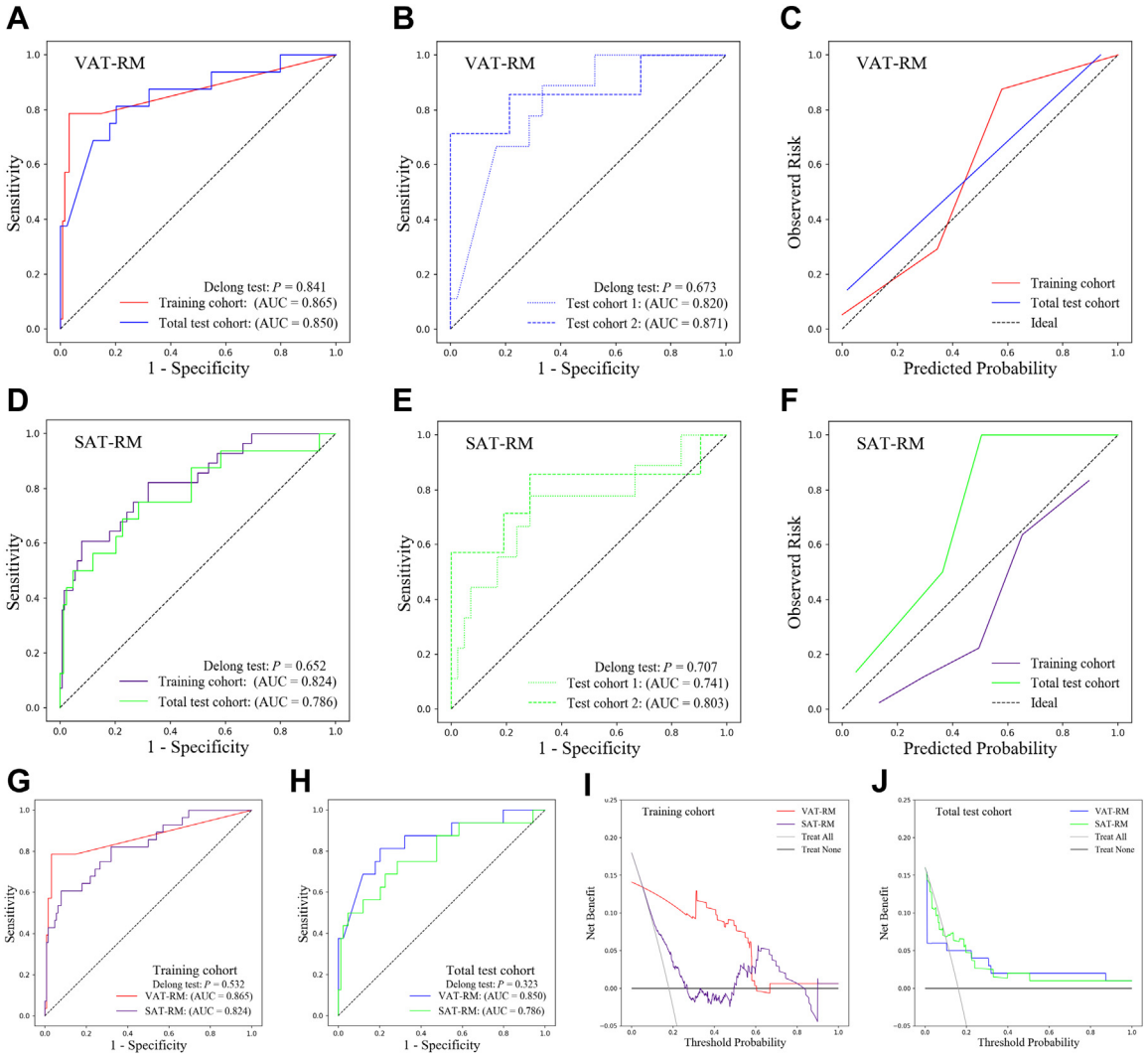

Fig. 2: Predictive performance of the RMs in the training and test cohorts (A–F). Plots show the ROC curves for the VAT-RM in the training and total test cohorts (A) and in test cohorts 1 and 2 (B). Plot (C) shows the calibration curves for the VAT-RM in the training and total test cohorts. Plots show the ROC curves for the SAT-RM in the training and total test cohorts (D) and in test cohorts 1 and 2 (E). Plot (F) shows the calibration curves for the SAT-RM in the training and total test cohorts. Comparison of the predictive performance between the VAT-RM and SAT-RM (G–J). ROC curves of the VAT-RM and SAT-RM in the training cohort (G) and the total test cohort (H). Decision curves of the VAT-RM and SAT-RM in the training cohort (I) and total test cohort (J). (AUC, area under the receiver operating characteristic curve; RM, radiomics model; ROC, receiver operating characteristic; SAT, subcutaneous adipose tissue; VAT, visceral adipose tissue).

the era of medical artificial intelligence, these metrics, although limited, may have been the best options to assess adipose tissue at that time. Currently, artificial intelligence has distinguished itself in clinical support systems. Radiomics has enabled the comprehensive extraction of multidimensional information of VAT; hence, our VAT-RM achieved higher prediction efficacy.

Our study had several strengths. First, to our best knowledge, this is the first radiomics study to evaluate the effect of the whole VAT on CD progression, although the specific pathophysiological significance of these radiomics features remains unclear since it is impossible to separate whole VAT from live patients for corresponding analysis. This novel method was more accurate and comprehensive than CT measurements of the local VAT because VAT distant from the inflamed intestines can also be affected by inflammation and display features similar to those adjacent to inflamed intestines.[23] Second, this multicentre study included patients living across the country, and the CT enterography images were acquired over a period of nearly 5 years, which addressed potential biases in practice patterns in different cities and offered a broad spectrum of

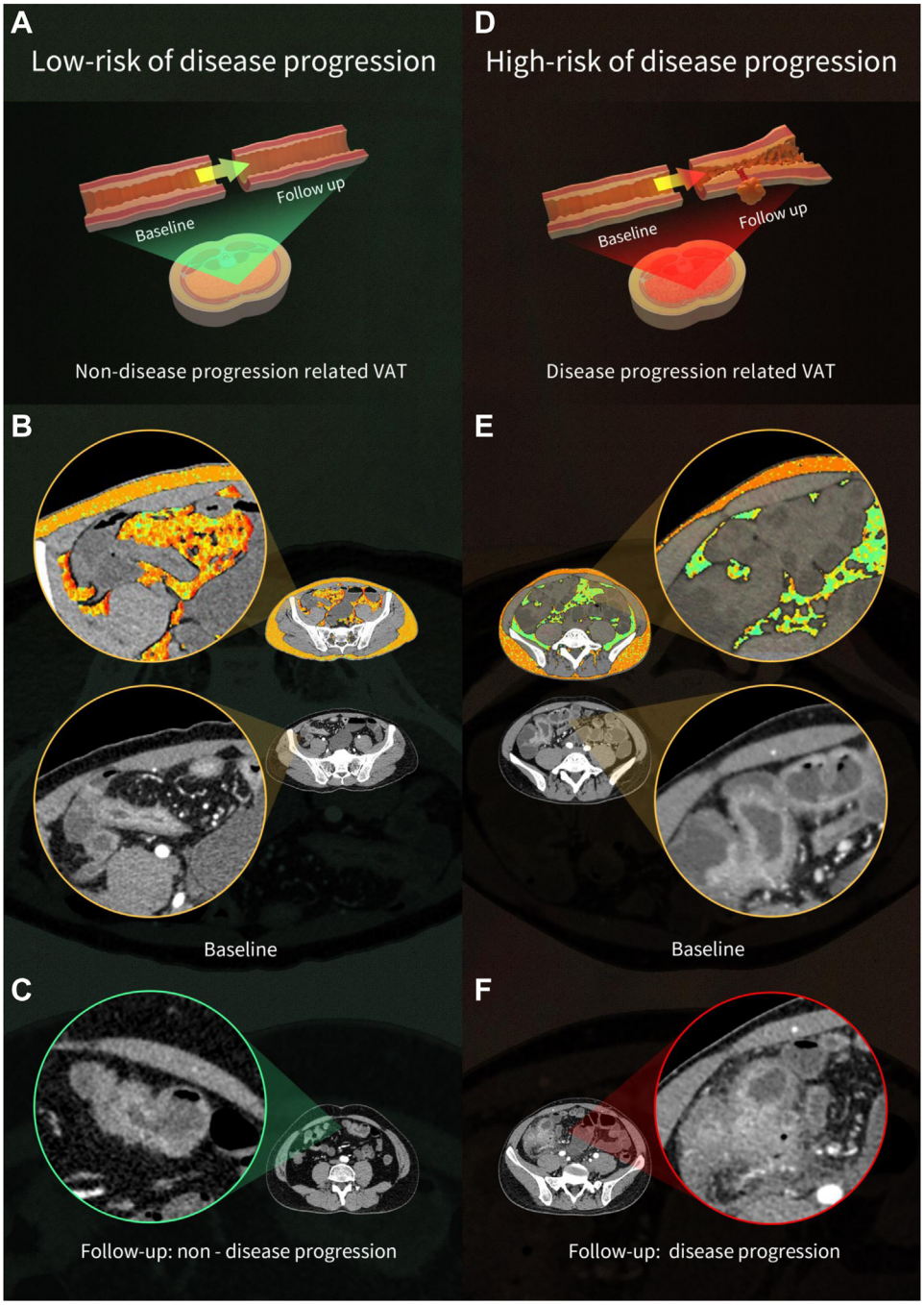

Fig. 3: Images showing representative patients with or without disease progression on relevant VAT and SAT radiomics feature maps overlaid on the CT images. Case 1 (A and B) involved a 40-year-old male patient with terminal ileal CD who demonstrated Montreal B1 at baseline and during the 26-month follow-up, while case 2 (D–F) involved a 25-year-old male patient with terminal ileal CD who demonstrated Montreal B1 at baseline but with penetrating disease during the 28-month follow-up. In each part, illustrations (A and D) show differences in VAT at baseline that affected bowel disease development during follow-up. Images (B and E) showing the representative radiomics features of adipose tissue (VAT: wavelet-HLL_glszm_LargeAreaLowGrayLevelEmphasis; SAT: wavelet-LHH_glszm_ZoneEntropy) overlaid on baseline plain CT images in these two patients; their terminal ileal CD is clearer on contrast-enhanced CT images. On the colour maps of radiomics features, these two patients showed a significant difference in VAT but not in SAT, indicating that VAT plays a more important role than SAT in disease progression in CD. Contrast-enhanced images (C and F) confirm the clinical outcomes of the two patients during follow-up. (CD, Crohn's disease; CT, computed tomography; SAT, subcutaneous adipose tissue; VAT, visceral adipose tissue).

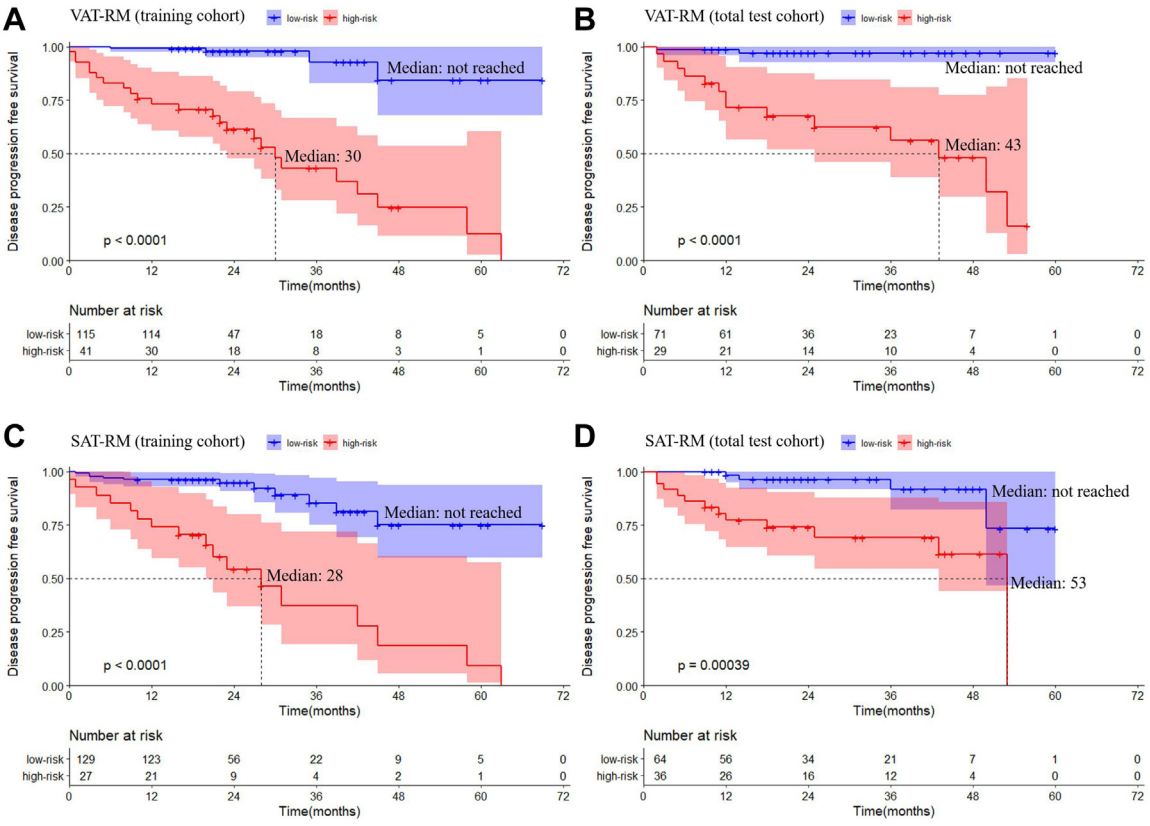

Fig. 4: Kaplan–Meier survival curves of disease progression-free survival for the VAT-RM in the training cohort (A) and total test cohort (B). The median value of the high-risk subgroup was 30 months and low-risk subgroup was not reached in the training cohort with a significant difference ($P < 0.0001$), and the median value of the high-risk subgroup was 43 months and low-risk subgroup was not reached in total test cohort with a significant difference ($P < 0.0001$). Kaplan–Meier survival curve of adverse outcome-free survival for the SAT-RM in the training cohort (C) and total test cohort (D). The median value of the high-risk subgroup was 28 months and low-risk subgroup was not reached in training cohort with a significant difference ($P < 0.0001$), and the median value of the high-risk subgroup was 53 months and low-risk subgroup was not reached in total test cohort with a significant difference ($P = 0.0004$). (RM, radiomics model; SAT, subcutaneous adipose tissue; VAT, visceral adipose tissue).

patient diversity. Moreover, the occurrence rate of disease progression in patients with CD in our study was similar to that of another reported study with a similar duration of follow-up,[29] indicating the representation of our included population. Our VAT-RM showed remarkable robustness in prediction performance among these centres, indicating good reliability and generalisation.

Although this study touched on a relatively unexplored field, some limitations require consideration. First, this study was retrospective in nature, which limited the possibility of the dynamic display of VAT radiomics features, given the dynamic nature of VAT and bowel inflammation. Second, we did not include intestinal radiomics features for analysis since the inclusion of time-consuming precise bowel segmentation will reduce the clinical practicability. Our strict inclusion criteria had already limited the baseline disease behaviour to Montreal B1 for all patients, and the differences in laboratory factors such as CRP levels, which characterise bowel disease activities between patients with different outcomes at baseline, were not significant. Therefore, we speculate that our results will not change significantly even after including intestinal radiomics signatures. Third, due to the retrospective nature of this study, some potential predictors such as baseline faecal calprotectin[29] were unable to be included for comparison with VAT-RM, and the prediction value of the VAT-RM for biochemical disease progression and the escalation of medication use could not be estimated. Lastly, the sample size in this study was limited. In future prospective studies, data collection from more centres could sufficiently increase the sample size to address those unexplored issues.

In conclusion, VAT is an important determinant of disease progression in patients with CD. Our VAT-RM allows the accurate identification of high-risk patients who are prone to disease progression and offers notable

Characteristics	Training cohort		Test cohort	
	Hazard ratio	*P* value	Hazard ratio	*P* value
Univariate Cox proportional hazard analysis				
Clinical factors				
Sex	0.770 (0.359, 1.652)	0.503	1.924 (0.619, 5.983)	0.258
Age	1.008 (0.979, 1.037)	0.604	1.024 (0.992, 1.056)	0.139
Disease location	0.828 (0.635, 1.081)	0.165	1.23 (0.9450, 1.602)	0.124
Smoking	0.892 (0.402, 1.976)	0.778	1.181 (0.410, 3.403)	0.758
Disease duration (months)	1.003 (0.993, 1.013)	0.562	1.006 (0.996, 1.016)	0.226
BMI (kg/m^2)	0.900 (0.789, 1.027)	0.119	1.132 (0.972, 1.318)	0.112
Perianal fistula/abscess	1.560 (0.723, 3.364)	0.257	0.000 (0.000, Inf)	0.998
Drug history				
Biologics	2.213 (0.297, 16.51)	0.438	2.037 (0.557, 7.442)	0.282
Corticosteroids use 3 months ago	0.999 (0.298, 3.355)	0.999	0.548 (0.071, 4.219)	0.564
Immune preparations	0.802 (0.273, 2.351)	0.687	2.283 (0.637, 8.182)	0.205
Laboratory factors				
CRP (mg/L)	1.009 (0.995, 1.023)	0.199	1.004 (0.995, 1.013)	0.376
ESR (mm/h)	0.999 (0.986, 1.011)	0.851	1.003 (0.984, 1.022)	0.792
Albumin (g/L)	0.952 (0.887, 1.023)	0.179	0.923 (0.853, 0.999)	**0.047**
Hemoglobin (g/L)	0.990 (0.974, 1.005)	0.192	0.996 (0.975, 1.017)	0.688
Platelet (×10^9/L)	1.000 (0.997, 1.003)	0.868	0.999 (0.995, 1.003)	0.748
Adipose tissue metrics				
VAT volume	1.000 (1.000, 1.000)	0.700	1.000 (1.000, 1.000)	0.821
SAT volume	1.000 (1.000, 1.000)	0.781	1.000 (1.000, 1.000)	0.970
Visceral to subcutaneous fat volume ratio	1.072 (0.606, 1.895)	0.812	0.958 (0.865, 1.06)	0.408
Visceral to subcutaneous fat area ratio at L3	0.455 (0.174, 1.192)	0.109	0.876 (0.628, 1.221)	0.434
Visceral to subcutaneous fat area ratio at L4	0.589 (0.200, 1.731)	0.336	0.847 (0.511, 1.403)	0.518
Radiomic models				
VAT-RM	16.339 (5.649, 47.26)	**<0.001**	17.203 (3.890, 76.078)	**<0.001**
SAT-RM	7.516 (3.496, 16.16)	**<0.001**	6.072 (1.952, 18.889)	**0.002**
Multivariate Cox proportional hazard analysis				
VAT-RM	12.515 (3.897, 40.192)	**<0.001**	9.285 (1.962, 43.940)	**0.005**
SAT-RM	2.189 (0.896, 5.351)	0.086	3.280 (0.952, 11.300)	0.060
Albumin (g/L)	0.957 (0.860, 1.064)	0.415	0.899 (0.815, 0.993)	**0.036**

Bolded value of $P < 0.100$ was considered statistical significance for univariate Cox proportional hazard analysis. Bolded value of $P < 0.050$ was considered statistical significance for multivariate Cox proportional hazard analysis. BMI, body mass index; CRP, C-reactive protein; ESR, erythrocyte sedimentation rate; RM, radiomic model; SAT, subcutaneous adipose tissue; VAT, visceral adipose tissue.

Table 3: **Univariate and multivariate Cox proportional hazard analysis of clinical, laboratory, and imaging factors at baseline.**

advantages over the SAT-RM and conventional fat metrics. It can serve as a supplement to current risk stratification strategies at no extra expense, since CT examinations are performed in routine clinical practice.

Contributors

XHL, RM, BSH, and STF were responsible for the overall study design. XHL, CCH, NWZ, YQL, JQL, RYL, YDW, and JSH supervised the data collection. XHL, CCH, NWZ, YQL, JQL, RYL, YDW, ZLL, and JSH performed data analysis. XHL, CCH, NWZ, and YQL completed manuscript drafting. ZLL, JQL, EMC, XZZ, JPL, JHL, DPK, SST, YJZ, BH, CHS, MHC, BSH, RM, and STF were responsible for manuscript editing. All authors read, discussed, and approved the final version of the manuscript. All authors had full access to the data in the study and takes responsibility for the integrity of the data and the accuracy of the data analysis as well as the decision to submit for publication.

Data sharing statement

The data that support the findings of this study are available on request from the corresponding author Shi-Ting Feng.

Declaration of interests

All authors declare no competing interests.

Acknowledgements

This study was supported by the National Natural Science Foundation of China (82270693, 82070680, 82271958, 82072002, 81870451, 81970483, 82170537, 82222010), Guangdong Basic and Applied Basic Research Foundation (2020A1515010571), Shenzhen-Hong Kong Institute of Brain Science-Shenzhen Fundamental Research Institutions, China (2021SHIBS0003) and Young S&T Talent Training Program of Guangdong Provincial Association for S&T, China (GDSTA, No. SKXRC202202).

Appendix A. Supplementary data

Supplementary data related to this article can be found at https://doi.org/10.1016/j.eclinm.2022.101805.

References

1 Torres J, Mehandru S, Colombel JF, Peyrin-Biroulet L. Crohn's disease. *Lancet*. 2017;389(10080):1741–1755.
2 Singh S, Dulai PS, Zarrinpar A, Ramamoorthy S, Sandborn WJ. Obesity in IBD: epidemiology, pathogenesis, disease course and treatment outcomes. *Nat Rev Gastroenterol Hepatol*. 2017;14(2):110–121.
3 Coffey JC, Byrnes KG, Walsh DJ, Cunningham RM. Update on the mesentery: structure, function, and role in disease. *Lancet Gastroenterol Hepatol*. 2022;7(1):96–106.
4 Coffey CJ, Kiernan MG, Sahebally SM, et al. Inclusion of the mesentery in ileocolic resection for Crohn's disease is associated with reduced surgical recurrence. *J Crohns Colitis*. 2018;12(10):1139–1150.
5 Erhayiem B, Dhingsa R, Hawkey CJ, Subramanian V. Ratio of visceral to subcutaneous fat area is a biomarker of complicated Crohn's disease. *Clin Gastroenterol Hepatol*. 2011;9(8):684–687.
6 Li Y, Zhu W, Gong J, et al. Visceral fat area is associated with a high risk for early postoperative recurrence in Crohn's disease. *Colorectal Dis*. 2015;17(3):225–234.
7 Li XH, Feng ST, Cao QH, et al. Degree of creeping fat assessed by computed tomography enterography is associated with intestinal fibrotic stricture in patients with Crohn's disease: a potentially novel mesenteric creeping fat index. *J Crohns Colitis*. 2021;15(7):1161–1173.
8 Zuo L, Li Y, Zhu W, et al. Mesenteric adipocyte dysfunction in Crohn's disease is associated with hypoxia. *Inflamm Bowel Dis*. 2016;22(1):114–126.
9 Gillies RJ, Kinahan PE, Hricak H. Radiomics: images are more than pictures, they are data. *Radiology*. 2016;278(2):563–577.
10 Li X, Liang D, Meng J, et al. Development and validation of a novel computed-tomography enterography radiomic approach for characterization of intestinal fibrosis in Crohn's disease. *Gastroenterology*. 2021;160(7):2303–2316.
11 Shang J, Ma S, Guo Y, et al. Prediction of acute coronary syndrome within 3 years using radiomics signature of pericoronary adipose tissue based on coronary computed tomography angiography. *Eur Radiol*. 2022;32(2):1256–1266.
12 Yang M, Cao Q, Xu Z, et al. Development and validation of a machine learning-based radiomics model on cardiac computed tomography of epicardial adipose tissue in predicting characteristics and recurrence of atrial fibrillation. *Front Cardiovasc Med*. 2022;9:813085.
13 Ding Z, Wu XR, Remer EM, et al. Association between high visceral fat area and postoperative complications in patients with Crohn's disease following primary surgery. *Colorectal Dis*. 2016;18(2):163–172.
14 Ben-Horin S, Novack L, Mao R, et al. Efficacy of biologic drugs in short-duration versus long-duration inflammatory bowel disease: a systematic review and an individual-patient data meta-analysis of randomized controlled trials. *Gastroenterology*. 2022;162(2):482–494.
15 Selinger CP, Parkes GC, Bassi A, et al. A multi-centre audit of excess steroid use in 1176 patients with inflammatory bowel disease. *Aliment Pharmacol Ther*. 2017;46(10):964–973.
16 Kerur B, Machan JT, Shapiro JM, et al. Biologics delay progression of Crohn's disease, but not early surgery, in children. *Clin Gastroenterol Hepatol*. 2018;16(9):1467–1473.
17 Bruining DH, Zimmermann EM, Loftus EJ, Sandborn WJ, Sauer CG, Strong SA. Consensus recommendations for evaluation, interpretation, and utilization of computed tomography and magnetic resonance enterography in patients with small bowel Crohn's disease. *Gastroenterology*. 2018;154(4):1172–1194.
18 Rieder F, Bettenworth D, Ma C, et al. An expert consensus to standardise definitions, diagnosis and treatment targets for antifibrotic stricture therapies in Crohn's disease. *Aliment Pharmacol Ther*. 2018;48(3):347–357.
19 Uko V, Vortia E, Achkar JP, et al. Impact of abdominal visceral adipose tissue on disease outcome in pediatric Crohn's disease. *Inflamm Bowel Dis*. 2014;20(12):2286–2291.
20 Bamba S, Inatomi O, Takahashi K, et al. Assessment of body composition from CT images at the level of the third lumbar vertebra in inflammatory bowel disease. *Inflamm Bowel Dis*. 2021;27(9):1435–1442.
21 Ha C, Martin A, Sepich-Poore GD, et al. Translocation of viable gut microbiota to mesenteric adipose drives formation of creeping fat in humans. *Cell*. 2020;183(3):666–683.
22 Lichtenstein GR, Loftus EV, Isaacs KL, Regueiro MD, Gerson LB, Sands BE. Acg clinical guideline: management of Crohn's disease in adults. *Am J Gastroenterol*. 2018;113(4):481–517.
23 Zulian A, Cancello R, Micheletto G, et al. Visceral adipocytes: old actors in obesity and new protagonists in Crohn's disease? *Gut*. 2012;61(1):86–94.
24 Seminerio JL, Koutroubakis IE, Ramos-Rivers C, et al. Impact of obesity on the management and clinical course of patients with inflammatory bowel disease. *Inflamm Bowel Dis*. 2015;21(12):2857–2863.
25 Grillot J, D'Engremont C, Parmentier AL, et al. Sarcopenia and visceral obesity assessed by computed tomography are associated with adverse outcomes in patients with Crohn's disease. *Clin Nutr*. 2020;39(10):3024–3030.
26 Bryant RV, Schultz CG, Ooi S, et al. Obesity in inflammatory bowel disease: gains in adiposity despite high prevalence of myopenia and osteopenia. *Nutrients*. 2018;10(9):1192.
27 Igarashi Y, Tanaka M, Okada H, et al. Visceral adipose tissue quality was associated with nonalcoholic fatty liver disease, independent of its quantity. *Nutr Metabol Cardiovasc Dis*. 2022;32(4):973–980.
28 Kundel V, Lehane D, Ramachandran S, et al. Measuring visceral adipose tissue metabolic activity in sleep apnea utilizing hybrid (18)F-FDG PET/MRI: a pilot study. *Nat Sci Sleep*. 2021;13:1943–1953.
29 Plevris N, Fulforth J, Lyons M, et al. Normalization of fecal calprotectin within 12 months of diagnosis is associated with reduced risk of disease progression in patients with Crohn's disease. *Clin Gastroenterol Hepatol*. 2021;19(9):1835–1844.